Published in final edited form as:
Cell. 2008 July 11; 134(1): 37–47. doi:10.1016/j.cell.2008.05.049.

Highly efficient, functional engraftment of skeletal muscle stem cells in dystrophic muscles

Massimiliano Cerletti[1,3], **Sara Jurga**[1,3], **Carol A. Witczak**[2], **Michael F. Hirshman**[2], **Jennifer L. Shadrach**[1,3], **Laurie J. Goodyear**[2], and **Amy J. Wagers**[1,3,4]

[1]Section on Developmental and Stem Cell Biology, Joslin Diabetes Center, One Joslin Place, Boston, MA 02115

[2]Section on Metabolism, Joslin Diabetes Center, One Joslin Place, Boston, MA 02115

[3]Department of Stem Cell and Regenerative Biology, Harvard University, and Harvard Stem Cell Institute

SUMMARY

Satellite cells reside beneath the basal lamina of skeletal muscle fibers and include cells that act as precursors for muscle growth and repair. Although they share a common anatomical localization and typically are considered a homogeneous population, satellite cells actually exhibit substantial heterogeneity. We used cell surface marker expression to purify from the satellite cell pool a distinct population of skeletal muscle precursors (SMPs) that function as muscle stem cells. When engrafted into muscle of dystrophin-deficient *mdx* mice, purified SMPs contributed to up to 94% of myofibers, restoring dystrophin expression and significantly improving muscle histology and contractile function. Transplanted SMPs also entered the satellite cell compartment, renewing the endogenous stem cell pool and participating in subsequent rounds of injury repair. Together, these studies indicate the presence in adult skeletal muscle of prospectively-isolatable muscle-forming stem cells and directly demonstrate the efficacy of myogenic stem cell transplant for treating muscle degenerative disease.

INTRODUCTION

Skeletal muscle is a unique tissue, composed of highly specialized post-mitotic, multinucleated fibers that contract to generate force and movement. Muscle growth and repair depends on a specialized subset of myofiber-associated mononuclear cells called “satellite cells” (Mauro, 1961) that associate closely with mature muscle fibers. While normally quiescent (Schultz et al., 1978), satellite cells become activated by muscle damage, which causes them to proliferate and differentiate to form fusion-competent myoblasts, which fuse with existing myofibers and one another to fully regenerate the muscle (reviewed in (Hawke and Garry, 2001; Wagers and Conboy, 2005)).

Satellite cells exhibit substantial phenotypic and functional heterogeneity, evident through differences in their cell surface marker expression, induction of myogenic transcription factors, and in vivo and in vitro proliferation characteristics (Beauchamp et al., 2000; Day et

[4]Address correspondence to amy.wagers@joslin.harvard.edu; Ph: (617) 732-2590; FAX (617) 732-2593..

al., 2007; Rouger et al., 2004; Sherwood et al., 2004a). However, the ability of skeletal muscle to undergo multiple rounds of regeneration throughout life while still maintaining the satellite cell pool suggests that at least a subset of satellite cells exhibits both self-renewal and differentiation capacities – hallmark properties of tissue stem cells (Wagers and Conboy, 2005).

Our previous work identified a unique combination of cell surface markers (CD45-Sca-1^{-}Mac-1^{-}CXCR4^{+}β1-integrin^{+}, abbreviated CSM4B), that prospectively identify autonomously myogenic cells within the myofiber-associated satellite cell compartment of adult mouse skeletal muscle and allow their direct isolation by fluorescence activated cell sorting (FACS) (Sherwood et al., 2004a). By marker enrichment analysis, the CSM4B subset was the only population capable of robust, clonal myogenic differentiation in cell culture assays (Sherwood et al., 2004a), suggesting that these skeletal muscle precursor cells (SMPs) might represent a unique subset of canonical muscle satellite cells that could act as self-renewing precursors for adult skeletal muscle.

Here, we analyze the stem cell and regenerative properties of prospectively identified SMPs. We demonstrate that in uninjured muscle SMPs express markers of resting satellite cells (Pax7^{+}MyoD^{-}), and lack expression of activation and myogenic differentiation markers (MyoD and myosin heavy chain (MyHC)). Furthermore, SMPs exhibit robust myogenic differentiation potential, both in vitro and in vivo. Direct isolation and transplantation of SMPs enables extensive reconstitution of damaged skeletal muscle, in both immunocompetent dystrophin-deficient *mdx* mice and cardiotoxin-injured wild-type mice. Importantly, high level engraftment of transplanted SMPs in *mdx* animals shows therapeutic value – restoring defective dystrophin gene expression, improving muscle histology, and rescuing physiological muscle function. Moreover, in addition to generating mature muscle fibers, transplanted SMPs also re-seed the satellite cell niche and are maintained there such that they can be recruited to participate in future rounds of muscle regeneration.

Taken together, these data indicate that SMPs act as renewable, transplantable stem cells for adult skeletal muscle. The level of myofiber reconstitution achieved by these myogenic stem cells exceeds that reported for most other myogenic cell populations (Bachrach et al., 2006; Deasy et al., 2007; Dellavalle et al., 2007; Dezawa et al., 2005; Montarras et al., 2005; Qu-Petersen et al., 2002; Sampaolesi et al., 2003; Sherwood et al., 2004b) and leads to a striking improvement of muscle contraction function in SMP-treated muscles. These data thus provide direct evidence that prospectively-isolatable, lineage-specific skeletal muscle stem cells provide a robust source of muscle replacement cells and a viable therapeutic option for the treatment of muscle degenerative disorders.

RESULTS

SMPs are a subset of canonically defined satellite cells

Satellite cells are classically defined by their unique anatomical location – beneath the basal lamina and adjacent to the plasma membrane of mature muscle fibers. Satellite cells in resting muscle are largely quiescent (Mauro, 1961), and exhibit high level expression of early myogenic transcription factors, including the paired box (Pax) protein Pax7 and, in some muscles, Pax3 (reviewed in (Buckingham, 2006; Dhawan and Rando, 2005; Wagers and Conboy, 2005)). To better understand the relationship of FACS-sorted CSM4B SMPs to classically defined satellite cells, we analyzed their expression of myogenic transcription factors, and their cell cycle profile in the normal muscle of adult (8-16 wks. of age) C57BL mice.

When sorted directly from resting skeletal muscle (Figure S1), >90% of purified $CD45^-Sca\text{-}1^-Mac\text{-}1^-CXCR4^+\beta1\text{-integrin}^+$ (CSM4B) SMPs showed robust expression of nuclear-localized Pax7 protein (Figures 1A, C), a selective marker of primitive myogenic cells (Seale et al., 2000), while <5% expressed MyoD (Figure 1C), a myogenic transcription factor that is not expressed in quiescent satellite cells but can be reversibly induced upon satellite cell activation (Cornelison and Wold, 1997; Yablonka-Reuveni and Rivera, 1994; Zammit et al., 2004). 100% of sorted SMPs also co-stained for the surface receptors M-cadherin and Syndecan4, previously reported to be expressed by early myogenic precursor cells (Cornelison et al., 2001; Cornelison and Wold, 1997; Irintchev et al., 1994) (Figure S2A, B). As in previous studies of bulk satellite cells in adult limb muscles (Conboy and Rando, 2002; Montarras et al., 2005; Relaix et al., 2006), SMPs harvested fresh from pooled muscles exhibited varying levels of expression of the early myogenic transcription factor Pax3, measured by analysis of Pax3 reporter mice expressing *lacZ* under control of endogenous Pax3 promoter elements (Relaix et al., 2003) (Figures 1B, D). Significantly, sorted SMPs showed no detectable expression of markers of more differentiated muscle lineage cells, including desmin and myosin heavy chain (MyHC) (Figure 1C), although these markers were induced in *in vitro* differentiated daughter myocytes derived from clonally-sorted SMPs (Figure S3). Finally, cell cycle analysis of sorted SMPs, using the DNA intercalating fluorescent dye Hoechst 33342 (Ho) and the RNA binding probe, Pyronin Y (PY), which together provide a measure of cellular DNA content and transcriptional activity that is reflective of cell cycle position (Passegue et al., 2005), indicated that <1% of CSM4B SMPs in resting muscle are in S, G_2 or M phases of the cell cycle (i.e., exhibit >2N DNA content), and ~90-95% of SMPs are quiescent (in G_0) (Figure S2C, D).

Immunostaining of isolated myofibers indicated that $\beta1\text{-integrin}^+$ and $CXCR4^+$ cells were clearly detectable beneath the laminin layer surrounding isolated myofibers (Figure 2A, top row). In addition, the majority (97 ± 1%) of myofiber-associated $\beta1\text{-integrin}^+$ cells were also $Pax7^+$ (Figures 2A, middle row, and 2B, top, purple bar). In contrast, only 30 ± 5% of $CXCR4^+$ cells on isolated myofibers co-expressed Pax7 (Figures 2A, bottom row, and 2B, top, green bar). (Direct co-staining of CXCR4 and β1-integrin was not possible due to antibody incompatibility.) These data are consistent with our previous observations (Sherwood et al., 2004a), and indicate that CXCR4, while insufficient on its own to enrich for primitive myogenic cells, provides further enrichment of $Pax7^+$, muscle-forming precursors when combined with β1-integrin ((Sherwood et al., 2004a) and Figure S1). Significantly, ~90% of myofiber-associated $Pax7^+$ cells co-expressed β1-integrin and ~80% co-expressed CXCR4 (Figures 2A and 2B, bottom, blue and orange bars), supporting the notion that CXCR4 and β1-integrin mark a distinct subset of $Pax7^+$ satellite cells. Taken together, these data demonstrate that CSM4B SMPs indeed localize to the canonical sublaminar satellite cell niche and exhibit hallmark properties of undifferentiated myogenic precursor cells, including Pax7 and Pax3 expression (Figure 1) and the capacity to autonomously generate differentiated myocytes in clonal, myogenic cultures (Figure S3 and (Sherwood et al., 2004a)).

Mdx mice exhibit decreased endogenous frequencies of SMPs

Given their relatively undifferentiated phenotype and robust myogenic activity *in vitro*, we predicted that CSM4B SMPs might be effective mediators of muscle repair in cell transplantation strategies. To test this hypothesis, we made use of the *mdx* mouse model, which harbors a mutation in the *dystrophin* gene (*Dys*) that results in the absence of dystrophin protein on the majority of muscle cell membranes (Figure 3A and (Lu et al., 2000; Sicinski et al., 1989; Wernig et al., 2005)). Loss of dystrophin expression reduces the structural integrity of *mdx* muscle fibers (reviewed in (Durbeej and Campbell, 2002)),

resulting in repeated cycles of muscle degeneration and regeneration that have been suggested to invoke a continual need for satellite cell proliferation and cause premature loss or impairment of myogenic activity (Blau et al., 1983; Heslop et al., 2000; Luz et al., 2002; Wright, 1985). Interestingly, dystrophic disease in *mdx* animals results in a significantly reduced *in vivo* representation of myogenic CSM4B SMPs within the myofiber-associated cell compartment. This decrease in SMP frequency is detectable as early as 12 wks. of age (Figure 3B, C), likely reflecting a detrimental effect of dystrophy on maintenance of the muscle precursor population. However, consistent with previous reports (Yablonka-Reuveni and Anderson, 2006), sorted *mdx* SMPs exhibited equivalent in vitro myogenic colony forming activity and efficient differentiation capacity (Figure 3D, E).

Transplanted SMPs robustly engraft muscle in vivo

To test the capacity of prospectively sorted SMPs to engraft in diseased muscle and to act as a regenerative precursor population to repair dystrophic muscle, we purified green fluorescent protein (GFP)-expressing CSM4B SMPs (Figure S4) from pooled limb muscles (including EDL, TA, gastrocnemius, quadriceps, soleus and triceps brachii) of β-actin/GFP transgenic mice (Wright et al., 2001) and injected these directly into the dystrophic muscle of 12-15 wk. old *mdx* mice (which do not express GFP and show only low numbers of dystrophin$^+$ revertant fibers, Figure 3 and (Sicinski et al., 1989)). Recipient *mdx* animals in these experiments were pre-injured by intramuscular injection of cardiotoxin one day prior to transplant in order to enhance the muscle regenerative response (Sherwood et al., 2004a) (Figure 4A). Engraftment of donor-derived myofibers in *mdx* recipients was measured by direct epifluorescence (for GFP) and indirect immunofluorescence (for dystrophin) on transverse sections of muscle harvested 4 wks. after transplant. (GFP detection by epifluorescence also was confirmed by indirect immunofluorescence and immunohistochemistry, see Figure S5.). Analyses of transplanted TA and gastrocnemius muscles of recipient mice revealed a robust, dose-dependent engraftment of donor-derived GFP$^+$ myofibers (Figure 4B, C). Donor-engrafted GFP$^+$ myofibers showed centrally localized nuclei (Figure 4C), characteristic of newly regenerated myofibers, and the majority (85-100%) stained positively for dystrophin protein on the myofiber membrane (Figures 4C, D). Additional experiments suggested that transplanted SMPs contribute to muscle regeneration both by fusion with existing myofibers and endogenous myocytes, and by *de novo* myogenesis. GFP$^+$ SMPs were transplanted into the muscle of related transgenic mice constitutively expressing a distinct fluorescent marker (HcRed). Because all skeletal muscle fibers in HcRed transgenic mice express HcRed (Sherwood et al., 2004b), this transplant strategy directly discriminates autonomously formed donor myofibers (GFP$^+$HcRed$^-$) from host fibers (GFP$^-$HcRed$^+$), and from hybrid fibers (GFP$^+$HcRed$^+$) formed by fusion of GFP$^+$ precursors with HcRed$^+$ host myofibers. Engrafted muscles from HcRed recipients showed all three myofiber types (Figure S6A), indicating that transplanted SMPs both fuse with existing host myocytes and myofibers and generate myofibers *de novo*.

Using the data shown in Figure 4B, we estimated the efficiency with which transplanted SMPs contribute to regenerating myofibers by calculating the regeneration index (RI), defined as the number of donor-engrafted myofibers generated per 10^5 transplanted cells (Deasy et al., 2007). This calculation yielded an RI of 3726 ± 272 for freshly isolated SMPs, which is ~5 to 40-fold higher than RIs estimated similarly from previous reports of cultured populations of muscle-derived stem and progenitor cells (Bachrach et al., 2006; Deasy et al., 2007; Montarras et al., 2005; Qu-Petersen et al., 2002) or non-muscle lineage cells (Dellavalle et al., 2007; Dezawa et al., 2005; Sampaolesi et al., 2003; Sherwood et al., 2004b), and roughly equivalent to myogenic cells identified using genetically-modified mice expressing a Pax3 reporter gene (Montarras et al., 2005). Other populations of myofiber-associated cells lacking expression of SMP markers do not exhibit this robust in vivo

engraftment capacity (Figures 4E, F and (Sherwood et al., 2004a)). SMP-derived myofibers were maintained in *mdx* hosts for up to 4 months post-transplant (the longest timepoint analyzed, data not shown).

SMP engrafted muscles show significant improvement in contraction function

To test whether engraftment by wild-type cells and restoration of dystrophin expression might have a therapeutic benefit for engrafted *mdx* muscles, we measured muscle force production in previously transplanted *mdx* muscle as compared to mock-transplanted muscle. 20,000 FACS-sorted GFP^+ SMPs were transplanted into one uninjured soleus muscle of each of 16 *mdx* recipients, while the contralateral muscle of each recipient received PBS alone. Four weeks after transplant, intact SMP-transplanted and mock-transplanted muscles from individual *mdx* recipient mice were harvested and electrically stimulated to contract for 10 min. For each individual animal, the contraction forces of SMP-transplanted vs. mock-transplanted muscles were measured in parallel. To compare contraction forces, the Peak Specific Force (a measure of the initial strength of muscle contraction) and Integrated Area Under the Curve (contraction amplitude X duration, a measure that takes into account the muscle's initial strength as well as resistance to fatigue) were calculated (Table S1). The fold differences in these values for SMP-transplanted vs. mock-transplanted muscle of the same animal were used for correlation analyses. These studies revealed a striking and significant ($P<0.001$) correlation between muscle force production and the degree of engraftment from transplanted SMPs, with highly engrafted muscle – showing up to 94% GFP-expressing myofibers – exhibiting up to 5.5-fold greater force production as compared to mock-transplanted muscle in these assays (Figures 5B, C, and Table S1). Comparison to contraction forces measured independently for soleus muscles of normal, wild type mice that were age- and sex-matched to the transplant recipients revealed that engrafted *mdx* animals showing >25% GFP^+ fibers exhibited average Peak Specific Forces approaching those of non-dystrophic animals (29.5 ± 2.7 mN/mm^2 vs. 31.47 ± 7.06 (mean ± SEM) mN/mm^2). Interestingly, although donor SMPs for these experiments were purified primarily from “fast-twitch” muscle (containing predominantly type II myofibers), the engrafted fibers showed a mixed distribution of “fast-twitch” and “slow-twitch” (type I) fibers characteristic of the soleus muscle into which they were implanted (Figure S6B). These data confirm the dominance of the muscle environment in specifying fiber type (Collins et al., 2005), and rule out the possibility that a transplant-induced change in muscle fiber type is responsible for the improved muscle contraction force.

Taken together, these data clearly demonstrate the capacity of prospectively identified muscle-resident precursor cells to differentiate robustly and selectively to regenerate mature, functional myofibers when transplanted into injured or damaged muscle. Remarkably, in some animals, transplanted SMPs supported nearly complete chimerism of myofibers, and these highly engrafted muscles (typically those showing >25% GFP^+ myofibers) exhibited striking improvements in physiologic function (Figure 5). We observed widespread contributions of transplanted SMPs to mature muscle fibers, and improved histology in SMP engrafted muscles, both with and without cardiotoxin pre-treatment, indicating that highly ablative pre-conditioning is not necessary to achieve therapeutic muscle engraftment in dystrophic muscles (Figures 4, 5, and S7).

Transplanted SMPs functionally re-engraft the satellite cell niche

The robust regenerative activity of SMPs requires no intervening cell culture (Deasy et al., 2007; Dellavalle et al., 2007; Dezawa et al., 2005), or genetic manipulation (Dezawa et al., 2005; Kuang et al., 2007), and on a per cell basis appears to exceed the engraftment efficiencies of most previously described populations of muscle cells or other cell types (Bachrach et al., 2006; Deasy et al., 2007; Dezawa et al., 2005; Morgan et al., 1993; Qu-

Petersen et al., 2002; Wernig et al., 2005). However, an ideal cell for muscle therapy must also be capable of re-populating the precursor cell pool, providing an enduring source of regenerative cells for muscle repair after injury. We therefore tested the ability of transplanted SMPs to re-enter and renew within the satellite cell compartment and to be recruited for subsequent rounds of regenerative myogenesis. For these studies, *mdx* mice were pre-injured by cardiotoxin injection and transplanted with GFP^+ SMPs. Four weeks later, SMP-transplanted muscles, or mock-transplanted control muscles, were harvested and analyzed for engraftment of donor cells into the satellite cell compartment. Single myofibers harvested from engrafted recipients were stained for Pax7 to reveal myofiber-associated satellite cells on donor-engrafted (GFP^+) myofibers. Strikingly, the majority of $Pax7^+$ cells found on GFP^+ myofibers from previously transplanted *mdx* gastrocnemius and soleus muscles exhibited co-expression of GFP, indicating that most of the satellite cells on these myofibers derived from the previously transplanted SMPs (Figures 6A, B). In addition, FACS analysis of enzymatically-prepared myofiber-associated cells isolated from gastrocnemius and soleus muscles of grafted *mdx* mice showed a clearly distinguishable population of GFP^+ SMPs within previously transplanted *mdx* muscle (Figure 6C). Transplanted GFP^+ SMPs gave rise not only to cells that retained the SMP phenotype, but also generated $CXCR4^-\beta1\text{-integrin}^+$ and $CXCR4^-\beta1\text{-integrin}^-$ cells (Figure S9), suggesting that these represent the progeny of primitive SMPs. Finally, to assess the capacity of the engrafted SMP population to be recruited again to participate in subsequent rounds of muscle repair, we re-injured the muscles of *mdx* mice previously transplanted with GFP^+ SMPs by a second intramuscular injection of cardiotoxin, and compared the numbers of donor-derived (GFP^+) myofibers found in re-injured muscles to those found in previously transplanted muscles that were not re-injured. Consistent with ongoing participation of the engrafted donor cells in muscle repair and regeneration, re-injured muscles showed a significantly higher contribution of GFP^+ myofibers when compared to identically transplanted muscles that were not re-injured (Figure 6D). Taken together, these data clearly indicate that in vivo transplantation of prospectively identified SMPs not only allows reconstitution of mature muscle fibers, but also replenishes the primitive muscle precursor pool, thus seeding a reserve pool of muscle regenerative cells that can be recruited for subsequent rounds of muscle growth and repair.

DISCUSSION

Stem cells are present in many adult tissues, where they play an important role in postnatal growth and tissue regeneration. Our data in mice demonstrate that direct cell sorting using a distinct combination of cell surface markers allows the prospective identification of a novel subset of skeletal muscle satellite cells that exhibits properties of adult muscle stem cells. SMPs are committed myogenic precursor cells, isolated by negative selection for the cell surface markers CD45, Sca1, and Mac1 and positive selection for β1-integrin and CXCR4. Unlike previous approaches (Dezawa et al., 2005; Kuang et al., 2007; Montarras et al., 2005; Sampaolesi et al., 2003), isolation of SMPs is based on normally expressed cell surface markers, and therefore is broadly applicable to accomplish direct muscle stem cell isolation and analysis from different mouse strains and ages without the need for specialized transgenic lines or extended periods of cell culture.

To examine the therapeutic potential of SMPs, we conducted transplant studies into *mdx* mice, a model of Duchenne Muscular Dystrophy. Wild-type GFP^+ SMPs contributed robustly to the regeneration of mature muscle fibers in recipient mice at a frequency that was directly proportional to the number of precursor cells injected and that in some recipients approached complete donor chimerism for myofibers (Figure 5). Engraftment of wild-type SMPs into *mdx* muscle thus provides a highly effective mechanism for the introduction of the dystrophin gene into dystrophin-deficient muscle, consequently restoring dystrophin

protein expression on the majority of myofibers (Figure 4), reducing muscle inflammation and fibrosis (Figure S7B), and significantly improving physiological muscle function (Figure 5).

In addition to participating in the repair of differentiated muscle fibers, transplanted SMPs also re-enter the satellite cell niche, contributing the majority of $Pax7^+$ cells found on donor-derived myofibers (Figure 6). These engrafted precursor cells could be recruited to participate again in the repair of future muscle injury (Figure 6D). The high level of contribution of donor GFP^+ SMPs to mature GFP^+ myofibers and to the pool of satellite cells associated with GFP^+ fibers likely reflects both unique, cell autonomous properties of the SMP population, as well as cell non-autonomous aspects of the transplant model. Specifically, the lower endogenous frequency of SMPs in *mdx* muscle (Figure 3) and the cytotoxic effects of cardiotoxin pre-treatment on SMP numbers (Figure S8), may lessen potential competition from endogenous cells during transplant and facilitate high level contribution of the introduced GFP^+ cells. Alternatively, cardiotoxin pre-treatment may induce or enhance production of SMP support factors, and provide a more conducive environment for myogenic engraftment. However, it is important to note that muscle engraftment by SMPs was not dependent on highly ablative pre-injury, as these cells also contributed at high efficiency (up to 94% of total myofibers) after transfer into uninjured muscle (Figures 5 and S7). In addition, recipient immunosuppression (Montarras et al., 2005) was not necessary for high level SMP engraftment or for maintenance of grafted fibers for up to 4 months (data not shown). Thus, robust donor cell engraftment can be achieved in fully immunocompetent animals and can be maintained for extended periods of time following SMP transplant in mice, which should encourage investigation of analogous strategies for cell replacement therapy in humans.

Taken together, these data demonstrate that, like hematopoietic stem cells in the bone marrow (Kondo et al., 2003), SMPs represent a transplantable population of tissue-specific stem cells that can undergo self-renewing proliferation as well as lineage-selective differentiation in response to injury. Notably, this capacity for enduring regenerative function is a unique activity of this distinct subset of primitive muscle stem cells, and is not provided by their more differentiated daughters (Figures 4E, F), a finding that helps to explain the modest clinical benefit observed in earlier studies employing transplantation of differentiated myoblasts for the treatment of muscle degenerative disease (Miller et al., 1997; Peault et al., 2007). Thus, even in tissues composed of typically very long-lived progeny – like the skeletal muscle – stem cells appear to exhibit specialized activities, uniquely providing robust engraftment and long-term contribution to tissue regeneration. While the singular properties of muscle stem cells that are critical for these important activities remain largely undiscovered (as is the case for most stem cell populations identified to date), stem cell-specific attributes, including their ability to generate large numbers of progeny, their extensive self-renewal potential, or other more poorly understood characteristics (such as their ability to home to appropriate niches, or to sense environmental signals) likely promote their robust regenerative activity. The ability to prospectively identify and directly purify muscle stem cells (SMPs) from both normal and diseased skeletal myofibers will be a tremendous benefit for the future elucidation of both the normal processes that control muscle specification and the ways in which these processes are deregulated by disease. Such studies ultimately will build a molecular portrait of the positive and negative regulatory pathways controlling adult myogenesis, and will enable more refined interventions to enhance muscle function by restoring appropriate numbers and endogenous activity of these cells, which can be significantly perturbed by injury, disease and aging (Figure 3 and (Blau et al., 1983; Conboy et al., 2003; Conboy et al., 2005; Luz et al., 2002; Wright, 1985)). Finally, as demonstrated here, direct transplantation of highly purified muscle stem cells represents a promising therapeutic option for muscle degenerative

disorders, as these cells provide an effective source of immediately available muscle regenerative cells as well as a reserve pool that can maintain muscle regenerative activity in response to future challenges.

EXPERIMENTAL PROCEDURES

Mice

These studies used adult (8-16 weeks of age) C57BL/Ka mice, *mdx* mice (C57BL/10ScSn-Dmd^{mdx}, purchased from Jackson Laboratories, Bar Harbor, ME), FVB Pax3LacZ/+ heterozygous mice (Relaix et al., 2003), or GFP transgenic (C57BL/Ka-β-actin-EGFP (Wright et al., 2001)) or HcRed transgenic (C57BL/Ka-β-actin-HcRed (Sherwood et al., 2004a; Sherwood et al., 2004b)) mice, in which cytoplasmic GFP or HcRed, respectively, is expressed from the ubiquitous chicken β-actin promoter. Mice were maintained at the Joslin Diabetes Center and Harvard School of Public Health animal facilities according to institutionally approved protocols.

Single myofiber and SMP isolation

Single myofibers and myofiber-associated cells were prepared from intact limb muscles (EDL, gastrocnemius, quadriceps, soleus, TA, and triceps brachii), essentially as described (Conboy et al., 2003; Sherwood et al., 2004a). After isolation, myofiber-associated cells were stained for isolation by FACS of particular cell populations (see below). Markers for SMP isolation were CD45$^-$Sca-1$^-$Mac-1$^-$CXCR4$^+$β1-integrin$^+$ (Sherwood et al., 2004a). We typically obtain ~50,000 SMPs per gram of muscle from uninjured, 8-12 week old wild-type mice.

Flow cytometry

Flow cytometry analysis and cell sorting were performed at the Joslin Diabetes Center/ Harvard Stem Cell Institute Flow Cytometry Core. Both sorting and analysis were carefully optimized for antibody titration and to achieve maximal cell purity and viability. Staining was performed as in (Sherwood et al., 2004a). Antibody titrations and suppliers are available online in Supplemental Data.

Pax3 expression analysis

Sorted SMP cells or CD45$^+$ hematopoietic cells from Pax3LacZ/+ heterozygous mice were fixed in 4% paraformaldeyhyde and incubated overnight at 37°C with X-gal (Sigma) to determine LacZ expression.

Tissue injury

For injections into the TA and gastrocnemiuis muscles, anesthetized mice were injected with 25μl (0.03mg/ml) of *Naja mossambica mossambica* cardiotoxin (Sigma) 1 day before cell transplantation. The next day, double-sorted cells, in 5-10 μl PBS were injected directly into these pre-injured muscles. For soleus injections, muscles were not pre-injured before cell injection. The skin and fascia of anesthetized recipients were opened at the lateral aspect of the lower leg, and the gastrocnemius moved aside to expose the soleus for injection. Cells were delivered directly into the soleus, and the wound was closed with clips or suture. Injected TA, gastrocnemius, and soleus muscles were analyzed 4 wks. or 4 mo. after transplant.

Immunostaining

Staining of fixed (4% paraformaldeyhyde), frozen muscle sections (5-8μm thick) was performed as in (Sherwood et al., 2004a). GFP was detected microscopically by

epifluorescence, immunofluorescence, or immunohistochemistry. Sorted SMP cells were fixed in 4% paraformaldehyde, permeabilized in 0.2% Triton X-100/PBS (Sigma), then blocked and stained as for muscle sections. For immunostaining of individual myofibers, gastrocnemius and soleus muscles were harvested, fixed (4% paraformaldeyhyde, 1 hr.), and washed with PBS. Muscles were individually homogenized (T25 Basic tissue homogenizer, Kika Labortechnik, Staufen, Germany) at 8000 rpm in 15 ml PBS, replacing the fiber suspension every 15 seconds with fresh PBS. Isolated fibers were permeabilized with 0.2% Triton X-100/PBS, blocked with 50:50 MOM Blocking (Vector Labs) and 10% horse serum/5% non-fat dried milk/4% BSA in PBS, and stained as above, with the indicated antibodies. Antibody titrations, suppliers and details of staining are provided as Supplemental Data online.

Microscopy

Fluorescence and brightfield images were acquired using a standard Olympus BX60 microscope or Zeiss LSM 510 META confocal microscope (offering three visible wavelength lasers Argon/2 458, 477, 488, 514; HeNe1 543 and HeNe2 633; and two-photon capability, as well as META spectral emission detectors which can separate strongly overlapping fluorescence emission spectra). Standard fluorescence images were acquired using DP Manager (Olympus Optical CO, LTD), and confocal images were acquired using Zeiss LSM Image Browser. To confirm GFP signals and exclude autofluorescence artifacts, we conducted spectral analysis (as in (Jackson et al., 2004) and (Swenson et al., 2007)) on muscle sections and single isolated myofibers. Spectral images were acquired at 10.5 nm intervals from 477 nm to 702 nm, and confirmed that engrafted tissues showed intensity profiles characteristic of GFP (peaking at 509 nm), while control tissues exposed identically (pinhole 112 μm) showed no detectable fluorescence (data not shown).

Muscle force production

Mice were sacrificed by cervical dislocation, and soleus muscles rapidly excised. Resting muscle length was measured with a micrometer, and muscles attached to a tissue support with stimulating electrodes. Muscles were bathed in Krebs-Ringer-Bicarbonate buffer containing (in mM): 117 NaCl, 4.7 KCl, 2.5 $CaCl_2 \cdot 2H_2O$, 1.2 KH_2PO_4, 1.2 $MgSO_4 \cdot 7H_2O$, 24.6 $NaHCO_3$, 1.2 glucose and oxygen bubbled for 10 min. Optimal muscle length was determined for each muscle by increasing the resting tension in 0.2 g increments and applying a single electrical pulse generated by a Grass stimulator (Harvard Apparatus, Holliston, MA) (parameters: pulse rate = 1 pulse/s; duration = 1 ms; volts = 100 V). Force production was monitored using an isometric force transducer (Kent Scientific, Litchfield, CT), the converted digital signal captured by a data acquisition system (iWorx114, CB Sciences, Dover, NH), and assessed with analysis software (Labscribe, CB Sciences, Dover, NH). The resting tension at which peak force was achieved was the tension applied just prior to the muscle fatigue protocol.

Muscle force production was assessed by maximally stimulating muscles for 10 min (parameters: train rate = 2/min; train duration = 10 s; pulse rate = 100 pulses/s; duration = 0.1 ms; volts = 100 V). Specific force was calculated by normalizing force measurements to total muscle cross sectional area (CSA). Total CSA was determined by dividing muscle weight by the product of the muscle length and the average density of mammalian skeletal muscle (1.06 mg/mm^3). The average Peak Specific Force over the 10 min protocol, and the average Integrated Area Under the Curve (contraction amplitude × duration) over the 10 min protocol, were used separately for correlation analyses.

Statistical analysis

Results were assessed for statistical significance using Student's t test (Microsoft Excel) or by regression analysis (SigmaPlot 2000), as indicated.

Supplementary Material

Refer to Web version on PubMed Central for supplementary material.

Acknowledgments

We thank J. LaVecchio and G. Buruzula at Joslin DERC/Harvard Stem Cell Institute Flow Cytometry Core for excellent cell sorting, A. Pinkhasov in the Joslin DERC Advanced Microscopy Core for assistance with histology, P. Zhang at the Department of Biostatistics, Harvard School of Public Health for help with statistical analysis, L. Ding at the Harvard Neurodiscovery Center Optical Imaging Program for assistance with confocal microscopy, M. Loeken and F. Relaix for providing Pax3LacZ/+ mice, B. Olwin for providing anti-Syndecan4 antibody, and T. Serwold, I. Conboy, I. Weissman, T. Rando, and E. Gussoni for critical review of the manuscript. We also thank L. Zon, D. Melton, D. Montarras, and T. Partridge for helpful discussions throughout this study. This work was supported in part by a Burroughs Wellcome Fund career award (AJW), Seed and Program Grants from the Harvard Stem Cell Institute (AJW), and grants from the National Institutes of Health (R01DK068626 to LJG) and (F32AR051663 to CAW).

REFERENCES

Bachrach E, Perez AL, Choi YH, Illigens BM, Jun SJ, del Nido P, McGowan FX, Li S, Flint A, Chamberlain J, Kunkel LM. Muscle engraftment of myogenic progenitor cells following intraarterial transplantation. Muscle Nerve. 2006; 34:44–52. [PubMed: 16634061]

Beauchamp JR, Heslop L, Yu DS, Tajbakhsh S, Kelly RG, Wernig A, Buckingham ME, Partridge TA, Zammit PS. Expression of CD34 and Myf5 defines the majority of quiescent adult skeletal muscle satellite cells. J Cell Biol. 2000; 151:1221–1234. [PubMed: 11121437]

Blau HM, Webster C, Pavlath GK. Defective myoblasts identified in Duchenne muscular dystrophy. Proc Natl Acad Sci U S A. 1983; 80:4856–4860. [PubMed: 6576361]

Buckingham M. Myogenic progenitor cells and skeletal myogenesis in vertebrates. Curr Opin Genet Dev. 2006; 16:525–532. [PubMed: 16930987]

Collins CA, Olsen I, Zammit PS, Heslop L, Petrie A, Partridge TA, Morgan JE. Stem cell function, self-renewal, and behavioral heterogeneity of cells from the adult muscle satellite cell niche. Cell. 2005; 122:1–13. [PubMed: 16009123]

Conboy IM, Conboy MJ, Smythe GM, Rando TA. Notch-mediated restoration of regenerative potential to aged muscle. Science. 2003; 302:1575–1577. [PubMed: 14645852]

Conboy IM, Conboy MJ, Wagers AJ, Girma ER, Weissman IL, Rando TA. Rejuvenation of aged progenitor cells by exposure to a young systemic environment. Nature. 2005; 433:760–764. [PubMed: 15716955]

Conboy IM, Rando TA. The regulation of Notch signaling controls satellite cell activation and cell fate determination in postnatal myogenesis. Dev Cell. 2002; 3:397–409. [PubMed: 12361602]

Cornelison DD, Filla MS, Stanley HM, Rapraeger AC, Olwin BB. Syndecan-3 and syndecan-4 specifically mark skeletal muscle satellite cells and are implicated in satellite cell maintenance and muscle regeneration. Dev Biol. 2001; 239:79–94. [PubMed: 11784020]

Cornelison DD, Wold BJ. Single-cell analysis of regulatory gene expression in quiescent and activated mouse skeletal muscle satellite cells. Dev Biol. 1997; 191:270–283. [PubMed: 9398440]

Day K, Shefer G, Richardson JB, Enikolopov G, Yablonka-Reuveni Z. Nestin-GFP reporter expression defines the quiescent state of skeletal muscle satellite cells. Dev Biol. 2007; 304:246–259. [PubMed: 17239845]

Deasy BM, Lu A, Tebbets JC, Feduska JM, Schugar RC, Pollett JB, Sun B, Urish KL, Gharaibeh BM, Cao B, et al. A role for cell sex in stem cell-mediated skeletal muscle regeneration: female cells have higher muscle regeneration efficiency. J Cell Biol. 2007; 177:73–86. [PubMed: 17420291]

Dellavalle A, Sampaolesi M, Tonlorenzi R, Tagliafico E, Sacchetti B, Perani L, Innocenzi A, Galvez BG, Messina G, Morosetti R, et al. Pericytes of human skeletal muscle are myogenic precursors distinct from satellite cells. Nat Cell Biol. 2007; 9:255–267. [PubMed: 17293855]

Dezawa M, Ishikawa H, Itokazu Y, Yoshihara T, Hoshino M, Takeda S, Ide C, Nabeshima Y. Bone marrow stromal cells generate muscle cells and repair muscle degeneration. Science. 2005; 309:314–317. [PubMed: 16002622]

Dhawan J, Rando TA. Stem cells in postnatal myogenesis: molecular mechanisms of satellite cell quiescence, activation and replenishment. Trends Cell Biol. 2005

Durbeej M, Campbell KP. Muscular dystrophies involving the dystrophin-glycoprotein complex: an overview of current mouse models. Curr Opin Genet Dev. 2002; 12:349–361. [PubMed: 12076680]

Hawke TJ, Garry DJ. Myogenic satellite cells: physiology to molecular biology. J Appl Physiol. 2001; 91:534–551. [PubMed: 11457764]

Heslop L, Morgan JE, Partridge TA. Evidence for a myogenic stem cell that is exhausted in dystrophic muscle. J Cell Sci. 2000; 113(Pt 12):2299–2308. [PubMed: 10825301]

Irintchev A, Zeschnigk M, Starzinski-Powitz A, Wernig A. Expression pattern of M-cadherin in normal, denervated, and regenerating mouse muscles. Dev Dyn. 1994; 199:326–337. [PubMed: 8075434]

Jackson KA, Snyder DS, Goodell MA. Skeletal muscle fiber-specific green autofluorescence: potential for stem cell engraftment artifacts. Stem Cells. 2004; 22:180–187. [PubMed: 14990857]

Kondo M, Wagers AJ, Manz MG, Prohaska SS, Scherer DC, Beilhack GF, Shizuru JA, Weissman IL. Biology of hematopoietic stem cells and progenitors: implications for clinical application. Annu Rev Immunol. 2003; 21:759–806. [PubMed: 12615892]

Kuang S, Kuroda K, Le Grand F, Rudnicki MA. Asymmetric self-renewal and commitment of satellite stem cells in muscle. Cell. 2007; 129:999–1010. [PubMed: 17540178]

Lu QL, Morris GE, Wilton SD, Ly T, Artem'yeva OV, Strong P, Partridge TA. Massive idiosyncratic exon skipping corrects the nonsense mutation in dystrophic mouse muscle and produces functional revertant fibers by clonal expansion. J Cell Biol. 2000; 148:985–996. [PubMed: 10704448]

Luz MA, Marques MJ, Santo Neto H. Impaired regeneration of dystrophin-deficient muscle fibers is caused by exhaustion of myogenic cells. Braz J Med Biol Res. 2002; 35:691–695. [PubMed: 12045834]

Mauro A. Satellite cells of muscle skeletal fibers. J Biophys Biochem. 1961; 9:493–495.

Miller RG, Sharma KR, Pavlath GK, Gussoni E, Mynhier M, Lanctot AM, Greco CM, Steinman L, Blau HM. Myoblast implantation in Duchenne muscular dystrophy: the San Francisco study. Muscle Nerve. 1997; 20:469–478. [PubMed: 9121505]

Montarras D, Morgan J, Collins C, Relaix F, Zaffran S, Cumano A, Partridge T, Buckingham M. Direct isolation of satellite cells for skeletal muscle regeneration. Science. 2005; 309:2064–2067. [PubMed: 16141372]

Morgan JE, Pagel CN, Sherratt T, Partridge TA. Long-term persistence and migration of myogenic cells injected into pre-irradiated muscles of mdx mice. J Neurol Sci. 1993; 115:191–200. [PubMed: 7683332]

Passegue E, Wagers AJ, Giuriato S, Anderson WC, Weissman IL. Global analysis of proliferation and cell cycle gene expression in the regulation of hematopoietic stem and progenitor cell fates. J Exp Med. 2005; 202:1599–1611. [PubMed: 16330818]

Peault B, Rudnicki M, Torrente Y, Cossu G, Tremblay JP, Partridge T, Gussoni E, Kunkel LM, Huard J. Stem and progenitor cells in skeletal muscle development, maintenance, and therapy. Mol Ther. 2007; 15:867–877. [PubMed: 17387336]

Qu-Petersen Z, Deasy B, Jankowski R, Ikezawa M, Cummins J, Pruchnic R, Mytinger J, Cao B, Gates C, Wernig A, Huard J. Identification of a novel population of muscle stem cells in mice: potential for muscle regeneration. J Cell Biol. 2002; 157:851–864. [PubMed: 12021255]

Relaix F, Montarras D, Zaffran S, Gayraud-Morel B, Rocancourt D, Tajbakhsh S, Mansouri A, Cumano A, Buckingham M. Pax3 and Pax7 have distinct and overlapping functions in adult muscle progenitor cells. J Cell Biol. 2006; 172:91–102. [PubMed: 16380438]

Relaix F, Polimeni M, Rocancourt D, Ponzetto C, Schafer BW, Buckingham M. The transcriptional activator PAX3-FKHR rescues the defects of Pax3 mutant mice but induces a myogenic gain-of-function phenotype with ligand-independent activation of Met signaling in vivo. Genes Dev. 2003; 17:2950–2965. [PubMed: 14665670]

Rouger K, Brault M, Daval N, Leroux I, Guigand L, Lesoeur J, Fernandez B, Cherel Y. Muscle satellite cell heterogeneity: in vitro and in vivo evidences for populations that fuse differently. Cell Tissue Res. 2004; 317:319–326. [PubMed: 15322909]

Sampaolesi M, Torrente Y, Innocenzi A, Tonlorenzi R, D'Antona G, Pellegrino MA, Barresi R, Bresolin N, De Angelis MG, Campbell KP, et al. Cell therapy of alpha-sarcoglycan null dystrophic mice through intra-arterial delivery of mesoangioblasts. Science. 2003; 301:487–492. [PubMed: 12855815]

Schultz E, Gibson MC, Champion T. Satellite cells are mitotically quiescent in mature mouse muscle: an EM and radioautographic study. J Exp Zool. 1978; 206:451–456. [PubMed: 712350]

Seale P, Sabourin LA, Girgis-Gabardo A, Mansouri A, Gruss P, Rudnicki MA. Pax7 is required for the specification of myogenic satellite cells. Cell. 2000; 102:777–786. [PubMed: 11030621]

Sherwood RI, Christensen JL, Conboy IM, Conboy MJ, Rando TA, Weissman IL, Wagers AJ. Isolation of Adult Mouse Myogenic Progenitors; Functional Heterogeneity of Cells within and Engrafting Skeletal Muscle. Cell. 2004a; 119:543–554. [PubMed: 15537543]

Sherwood RI, Christensen JL, Weissman IL, Wagers AJ. Determinants of skeletal muscle contribution from circulating cells, bone marrow cells, and hematopoietic stem cells. Stem Cells. 2004b; 22:1292–1304. [PubMed: 15579647]

Sicinski P, Geng Y, Ryder-Cook AS, Barnard EA, Darlison MG, Barnard PJ. The molecular basis of muscular dystrophy in the mdx mouse: a point mutation. Science. 1989; 244:1578–1580. [PubMed: 2662404]

Swenson ES, Price JG, Brazelton T, Krause DS. Limitations of green fluorescent protein as a cell lineage marker. Stem Cells. 2007; 25:2593–2600. [PubMed: 17615263]

Wagers AJ, Conboy IM. Cellular and molecular signatures of muscle regeneration: current concepts and controversies in adult myogenesis. Cell. 2005; 122:659–667. [PubMed: 16143100]

Wernig G, Janzen V, Schafer R, Zweyer M, Knauf U, Hoegemeier O, Mundegar RR, Garbe S, Stier S, Franz T, et al. The vast majority of bone-marrow-derived cells integrated into mdx muscle fibers are silent despite long-term engraftment. Proc Natl Acad Sci U S A. 2005; 102:11852–11857. [PubMed: 16085712]

Wright DE, Cheshier SH, Wagers AJ, Randall TD, Christensen JL, Weissman IL. Cyclophosphamide/granulocyte colony-stimulating factor causes selective mobilization of bone marrow hematopoietic stem cells into the blood after M phase of the cell cycle. Blood. 2001; 97:2278–2285. [PubMed: 11290588]

Wright WE. Myoblast senescence in muscular dystrophy. Exp Cell Res. 1985; 157:343–354. [PubMed: 3979444]

Yablonka-Reuveni Z, Anderson JE. Satellite cells from dystrophic (mdx) mice display accelerated differentiation in primary cultures and in isolated myofibers. Dev Dyn. 2006; 235:203–212. [PubMed: 16258933]

Yablonka-Reuveni Z, Rivera AJ. Temporal expression of regulatory and structural muscle proteins during myogenesis of satellite cells on isolated adult rat fibers. Dev Biol. 1994; 164:588–603. [PubMed: 7913900]

Zammit PS, Golding JP, Nagata Y, Hudon V, Partridge TA, Beauchamp JR. Muscle satellite cells adopt divergent fates: a mechanism for self-renewal? J Cell Biol. 2004; 166:347–357. [PubMed: 15277541]

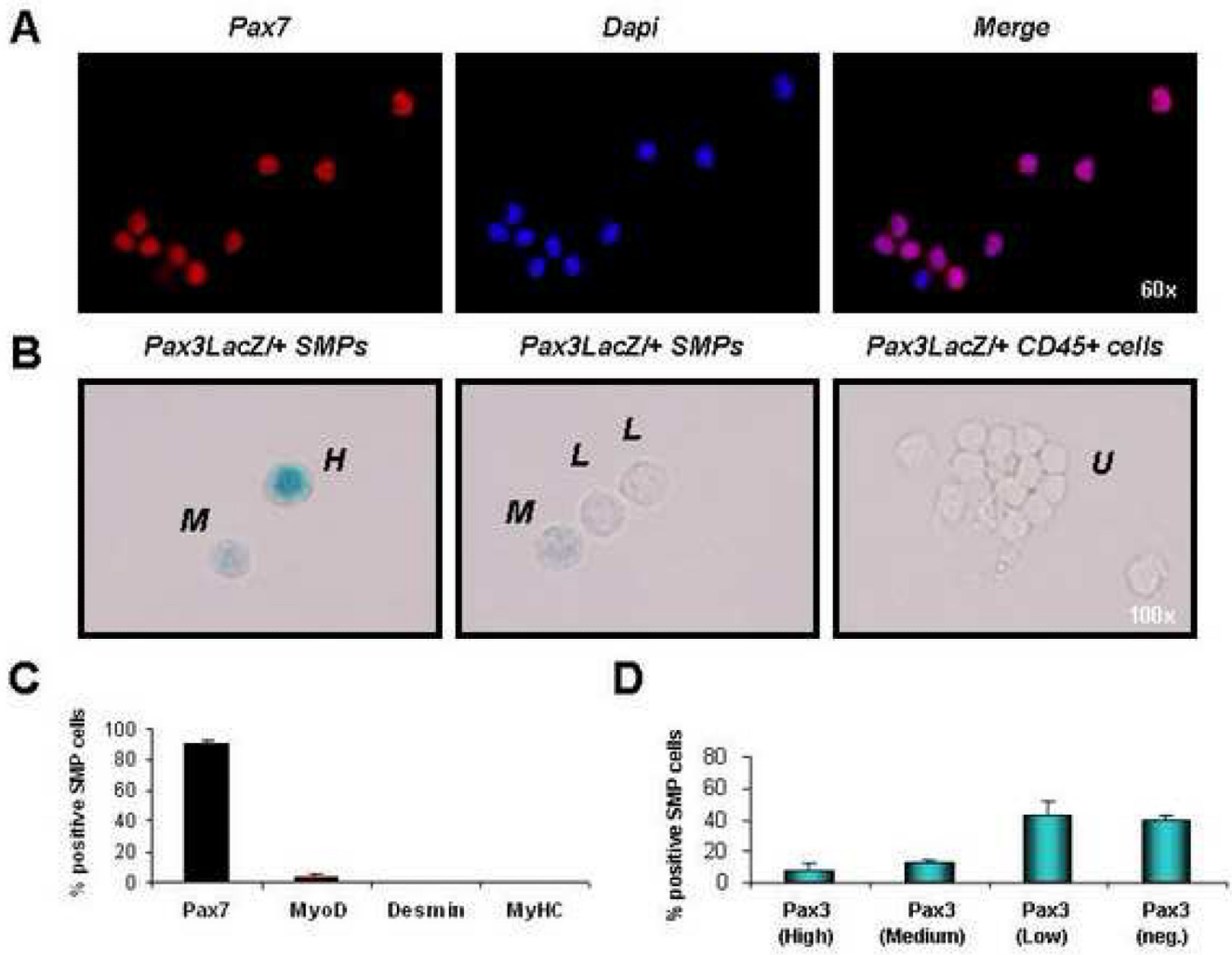

FIGURE 1. SMPs express markers of undifferentiated satellite cells

(**A**) Double-sorted SMPs (see Figures S1 and S4) were stained with antibody against Pax7. 90% (± 3.2%) of freshly sorted SMP cells showed nuclear Pax7 protein (red). Cell nuclei marked by DAPI (blue). (**B**) SMPs or $CD45^+$ hematopoietic cells (as a negative control) were sorted from pooled limb muscles (including EDL, TA, gastrocnemius, quadriceps, soleus, and triceps brachii) of adult $Pax3^{LacZ/+}$ heterozygous reporter mice, which express one copy of the bacterial β-galactosidase gene from the endogenous Pax3 promoter, providing a reliable reporter for Pax3 expression (Relaix et al., 2003). Double-sorted cells were stained with X-gal to detect LacZ activity and scored as high expressers (H, see left panel), medium expressers (M, see left and middle panels), low expressers (L, see middle panel), or undetectable (U, see right panels; cells were scored as undetectable if the level of X-gal staining was equivalent to background staining of the control $CD45^+$ cell population, which does not express Pax3 (data not shown)). (**C**) Freshly sorted SMPs were stained as in (A) with antibody against Pax7, MyoD, Desmin or MyHC. Most SMPs are $Pax7^+$, and <5% were $MyoD^+$. No expression of Desmin or MyHC was detected. (**D**) Quantification of Pax3 expression by sorted SMPs revealed heterogeneous levels of Pax3 expression, as expected based on previous studies (Montarras et al., 2005; Relaix et al., 2006). Data are presented as the frequency (Mean ± SD) of SMP cells exhibiting high, medium, low, or undetectable (neg.) LacZ activity.

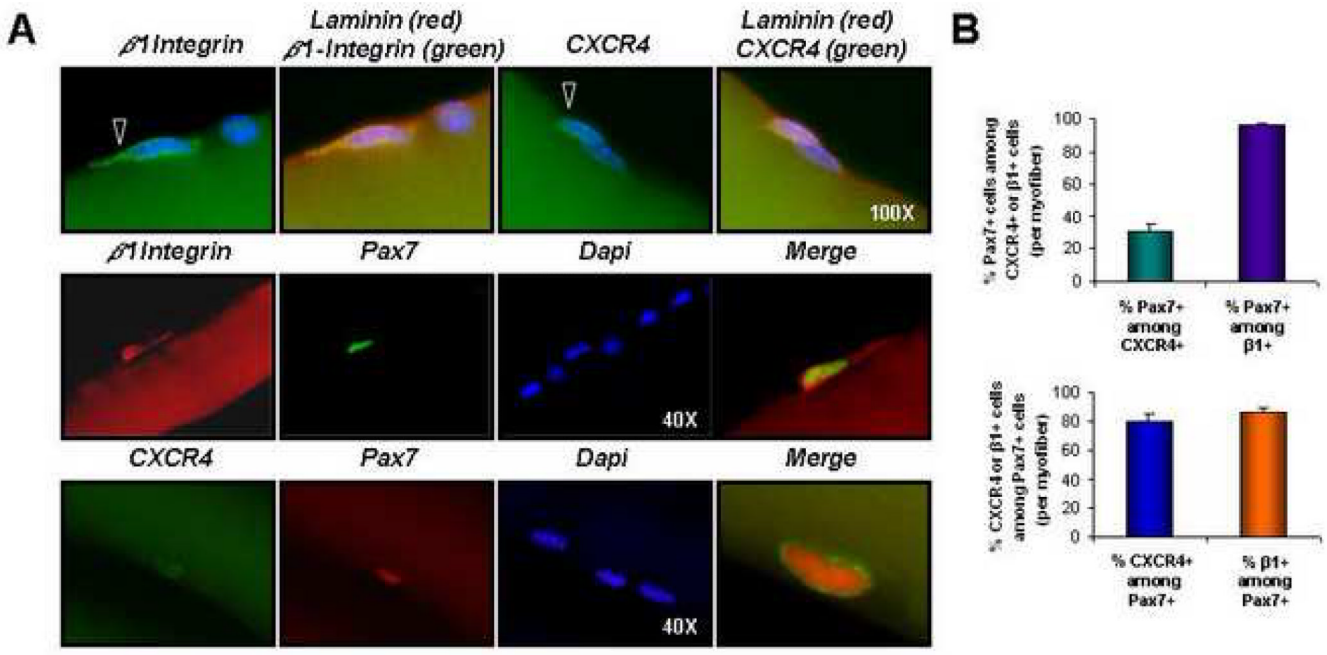

FIGURE 2. Expression of β1-integrin and CXCR4 by skeletal muscle satellite cells

(**A**) Single myofibers isolated from gastrocnemius or soleus muscles of C57BL mice were stained with anti-β1-integrin (green, top row, and red, middle row) or anti-CXCR4 (green, top and bottom rows) antibody, together with anti-laminin (red, top row) or anti-Pax7 (green, middle row and red, bottom row) and analyzed by fluorescence microscopy. Nuclei were marked by DAPI (blue). Open arrowheads denote β1-integrin$^+$ or CXCR4$^+$ cells (top row). Enlarged, merged images are shown at right (middle and bottom rows). (**B**) The average frequency of Pax7 and CXCR4 or Pax7 and β1-integrin co-expression by myofiber-associated cells was determined from analysis of 60 individual myofibers. Bar graphs depict the frequency of CXCR4-expressing (green) or β1-integrin-expressing (purple) myofiber-associated cells that also express Pax7 (Mean ± SEM), or the frequency of Pax7$^+$ cells that also express CXCR4 (blue) or β1-integrin (orange). The majority (80-90%) of Pax7$^+$ cells are also CXCR4$^+$ and β1-integrin$^+$ (bottom plot). Likewise, >90% of β1-integrin$^+$ cells are also Pax7$^+$, although only ~30% of CXCR4$^+$ cells co-express Pax7 (top plot). Based on flow cytometric analysis, CXCR4$^+$ cells that lack Pax7 expression appear for the most part to be CD45$^+$ infiltrating inflammatory cells (data not shown), which exhibit no myogenic activity.

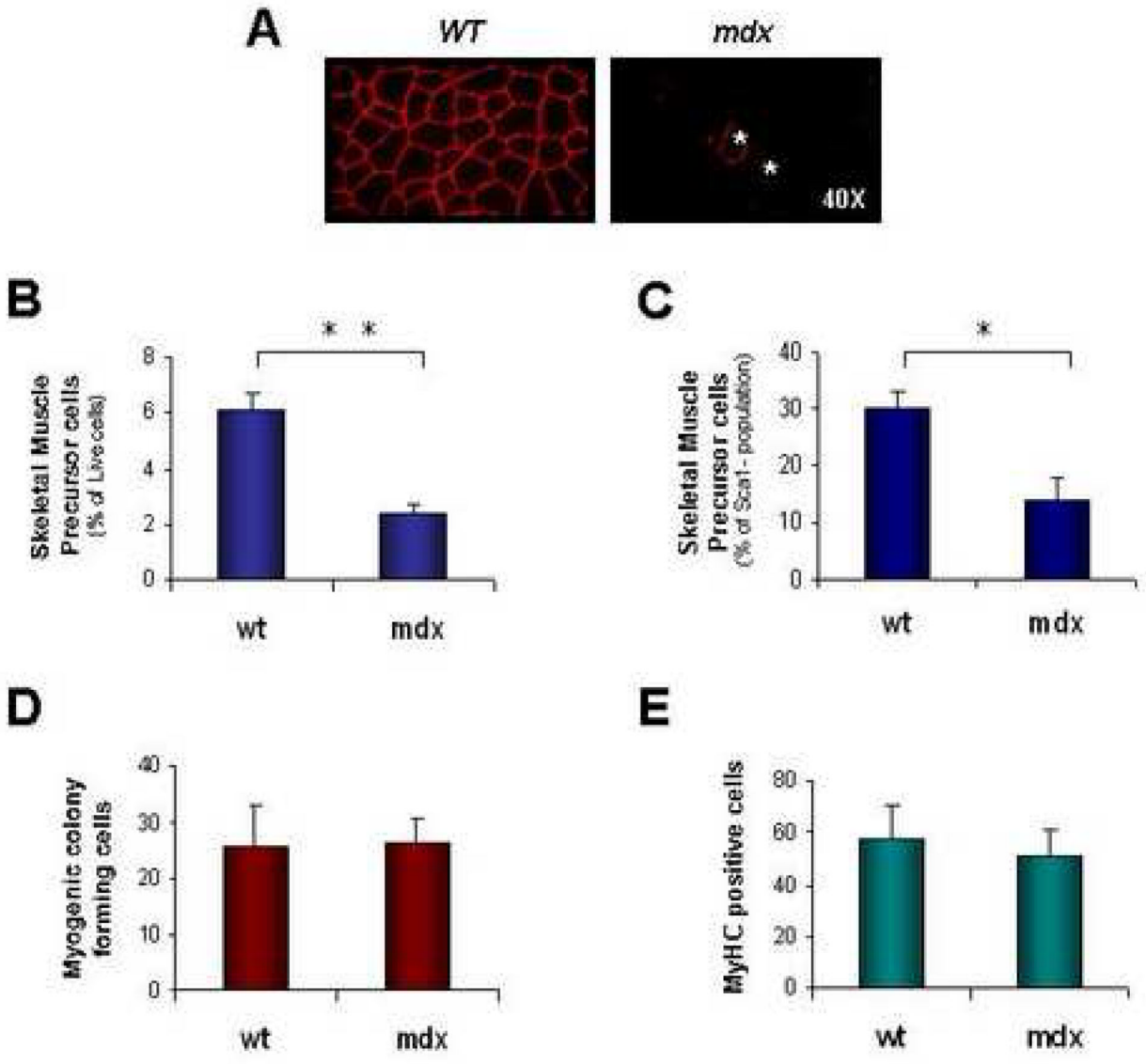

FIGURE 3. SMP frequency is reduced in dystrophic mice

Dystrophic disease in *mdx* animals is characterized by acute degeneration and regeneration of skeletal muscle during the first month of life, followed by a mild chronic dystrophy that begins at ~6-8 wks. of age and lasts throughout life. (**A**) Immunostaining for dystrophin protein in wild-type (wt) C57BL/Ka mice reveals protein expression at the cell membrane of every myofiber. In contrast, the majority of myofibers in *mdx* mice lack dystrophin expression, with the exception of a small number (~1-6% of total myofibers in mice aged 10-20 wks (Wernig et al., 2005)) of revertant fibers generated by skipping of the mutated exon (Lu et al., 2000). Two revertant fibers in the *mdx* muscle section shown are marked by asterisks (*). (**B** and **C**) Flow cytometric analysis of SMP frequency in dystrophic *mdx* mice shows an ~3-fold decrease in the frequency of SMPs among myofiber-associated cells (**B**) and an ~2-fold decrease among Sca-1$^-$ myofiber-associated cells (**C**) harvested from *mdx* muscle. *P<0.05, **P<0.01 (**D** and **E**) Double-sorted SMPs from *mdx* mice exhibited equivalent in vitro clonal plating efficiency (**D**, frequency of colony formation from single cells, as in Figure S3) and differentiation capacity (**E**, % of MyHC-expressing cells after

culture in differentiation medium, as in Figure S3) as compared to SMPs sorted from wild type (wt) mice.

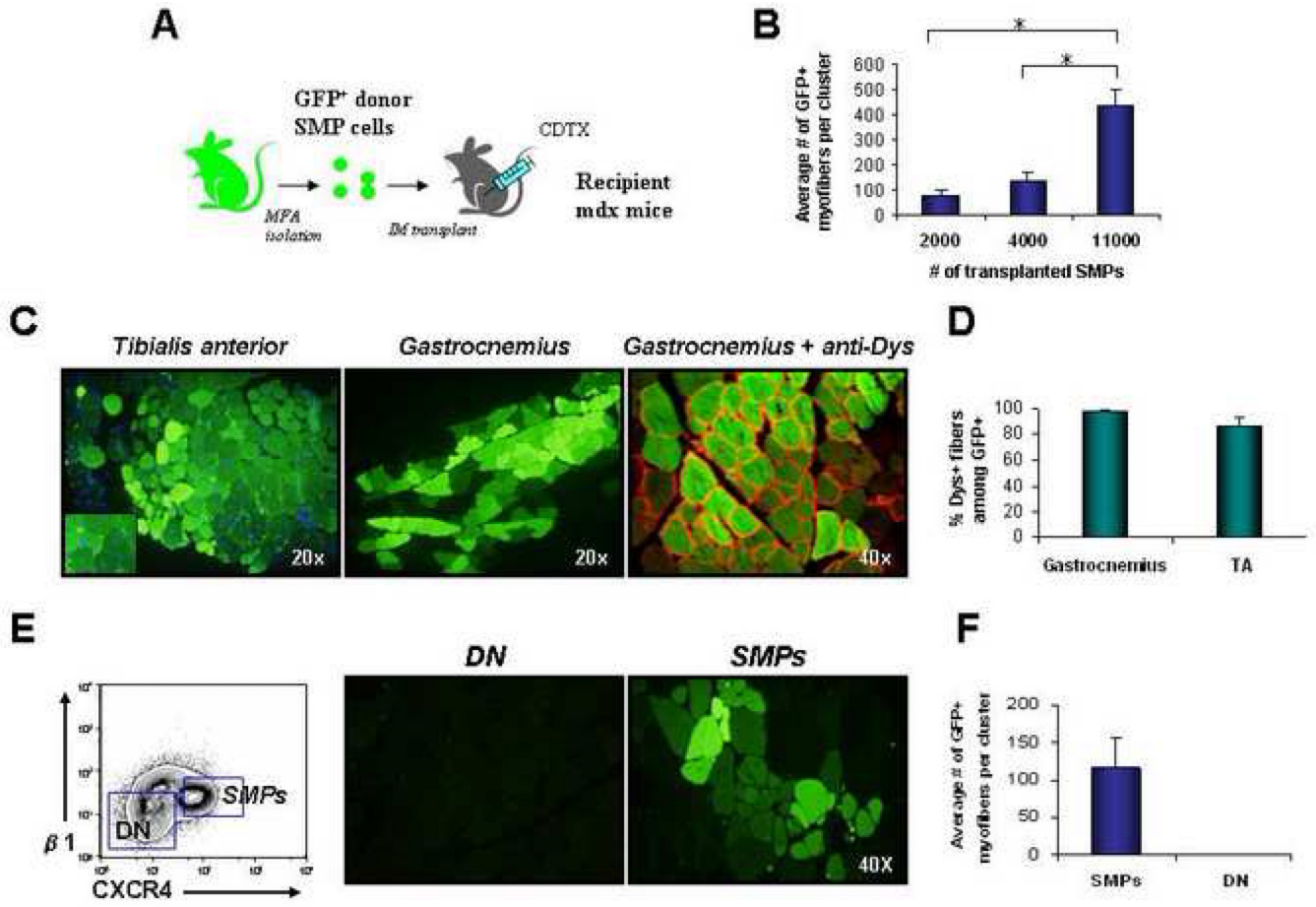

FIGURE 4. SMPs robustly engraft skeletal muscle in vivo

(**A**) Experimental design. Double-sorted GFP$^+$ SMPs were injected intramuscularly into recipient *mdx* mice injured 1 day previously by injection of cardiotoxin (CDTX) into the same muscle. (**B**) Quantitative analysis of donor-derived (GFP$^+$) myofibers in TA muscles injected with 2,000 (n=3), 4,000 (n=3) or 11,000 (n=3) SMPs. Recipient muscles were harvested 4 wks. after transplantation and analyzed for GFP expression by direct epifluorescence microscopy of transverse muscle sections. The total number of GFP$^+$ myofibers per section was determined for 100-300 sections taken throughout the muscle, in order to determine the maximal number of donor-derived fibers generated in each muscle. Data are plotted as the mean (± SEM) number of GFP$^+$ myofibers detected in the section of each engrafted muscle that contained the most GFP$^+$ myofibers. *P < 0.01. (**C**) Transverse frozen sections of TA (left panel) and gastrocnemius (middle and right panels) muscles obtained from *mdx* mice transplanted 4 wks. previously with 11,000 GFP$^+$ SMPs showed large clusters of regenerating donor-derived myofibers (GFP$^+$, shown in green) with characteristic centrally localized nuclei and restored dystrophin expression (shown in red; dystrophin staining is shown on the right image only). GFP detection by epifluorescence (as in C) was confirmed by indirect immunofluorescence and immunohistochemistry using anti-GFP antibodies (see Figure S5). (**D**) Quantification of the frequency (mean ± SD) of dystrophin$^+$ myofibers among GFP$^+$ donor-derived myofibers in the TA or gastrocnemius of *mdx* mice transplanted with 11,000 SMP cells per muscle, revealed that the majority (85-100%) of GFP$^+$ myofibers co-stained with dystrophin protein (red), which normally is lacking on most *mdx* myofibers ((Sicinski et al., 1989) and see Figure 3). (**E** and **F**)

Myofiber-associated cells lacking SMP markers do not generate myofibers when transplanted in vivo. CD45$^-$Sca-1$^-$Mac-1$^-$**CXCR4$^-$β1-integrin$^-$** (double negative, DN) cells or CD45$^-$Sca-1$^-$Mac-1$^-$**CXCR4$^+$β1-integrin$^+$** SMPs were twice-sorted (to ensure purity) from β-actin/GFP mice and then transferred at equal cell number (4000 per muscle) into separate pre-injured *mdx* recipients. Four weeks after transplant, injected muscles were harvested and sectioned. No GFP$^+$ myofibers were found in muscles transplanted with DN cells (n=3), while muscle receiving GFP$^+$ SMPs showed efficient contribution of GFP$^+$ myofibers (n=3).

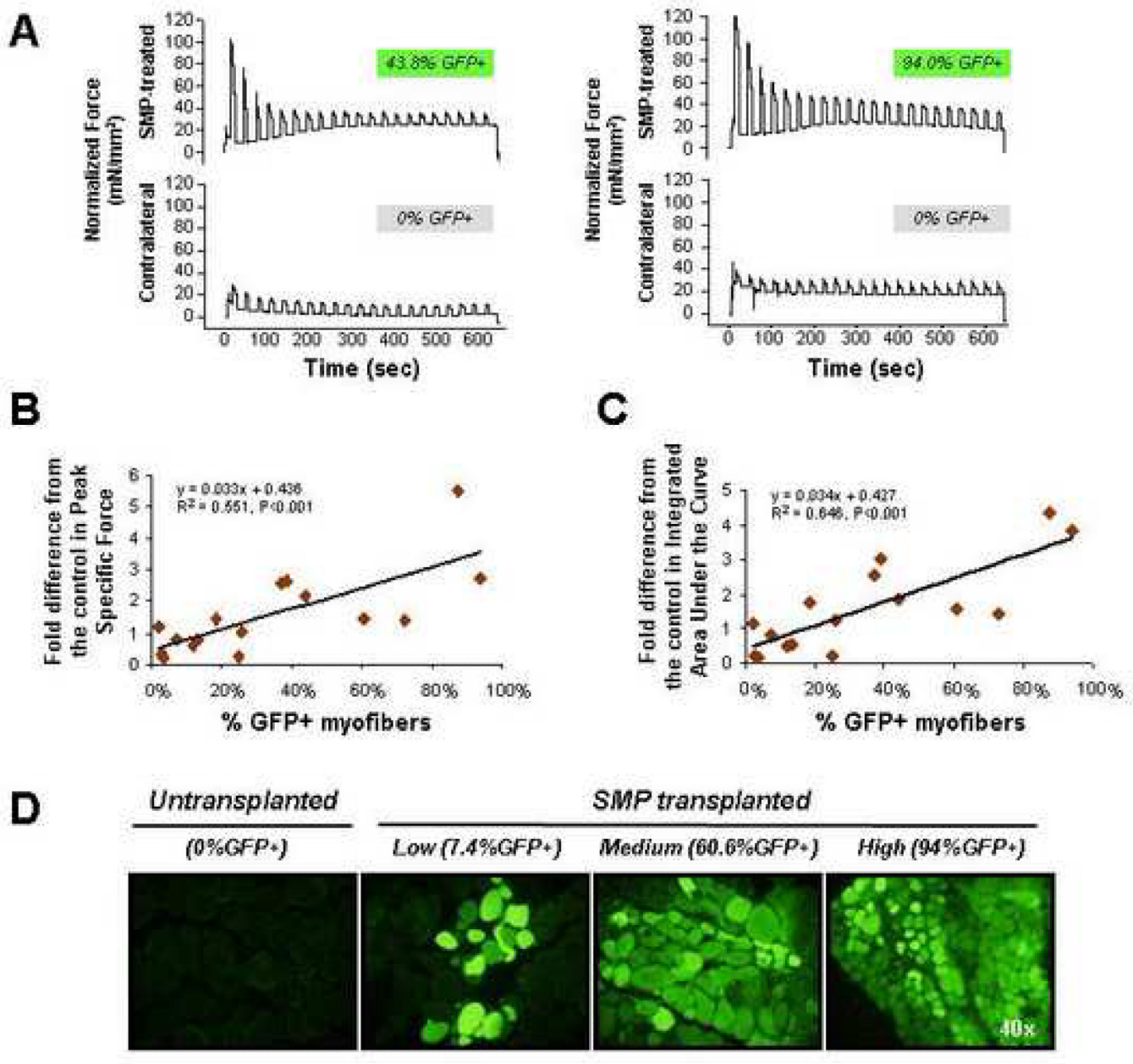

FIGURE 5. Functional improvement in muscle contractile force following engraftment of wild-type SMPs into dystrophic muscle

(**A**) Representative traces from contractile force measurements of SMP-transplanted (top rows) or mock-transplanted muscles. Traces are paired showing force production from contralateral muscles of the same recipient animal, and are normalized for muscle cross-sectional area. The % GFP^+ myofibers detected upon subsequent sectioning of each muscle is indicated above each trace. Normalized data for all animals in the study, used for calculation of the fold differences and regression curves shown in (**B** and **C**) are provided in Table S1. (**B**) Regression analysis shows a significant ($P<0.001$) correlation between the fold difference from the control in Peak Specific Force production for the 10 min contraction protocol (plotted as the ratio of the average peak specific force in SMP-transplanted vs. mock-transplanted, contralateral soleus muscle) and the % GFP^+ myofibers

in the transplanted muscle. Each diamond represents data from an individual mouse (n=16). (**C**) Regression analysis shows significant (P<0.001) correlation between the fold difference from the control in Integrated Area Under the Curve (amplitude X duration) for the 10 min contraction protocol (plotted as the average integrated area under the curve in SMP-transplanted vs. mock-transplanted, contralateral soleus muscle) and the % GFP^+ myofibers in the engrafted muscle. Each diamond represents an individual mouse (n=16). (**D**) Representative epifluorescence images showing GFP expression (green) in myofibers of mock-transplanted (left-most panel) or SMP-transplanted (three right panels) soleus muscles of individual *mdx* mice. Individual soleus muscles showed highly variable levels of engraftment, likely related to technical limitations in the efficiency of cell delivery that arise from the small size and less accessible anatomical location of the soleus.

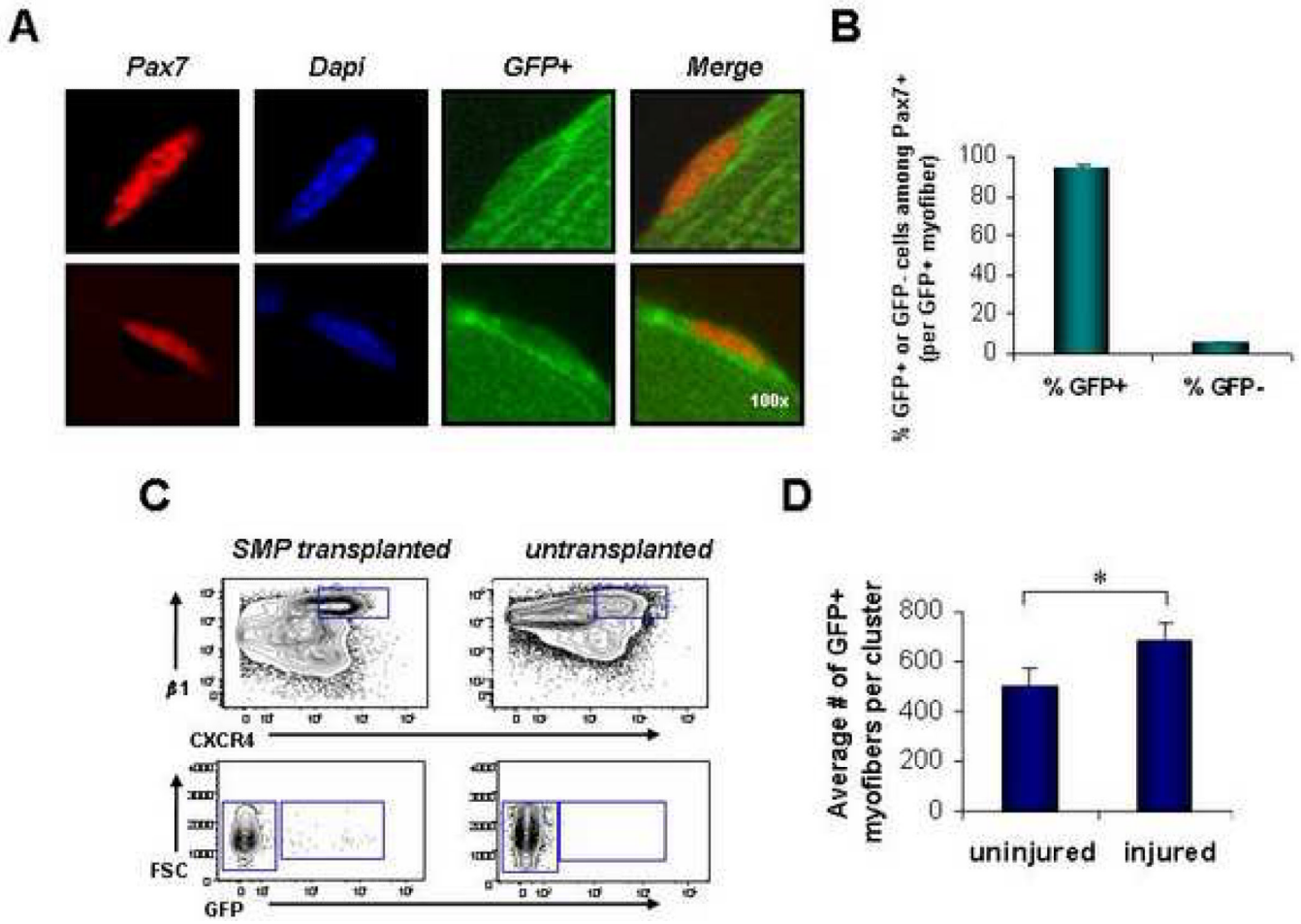

FIGURE 6. Transplanted SMPs re-seed the satellite cell compartment

(**A**) Intact myofibers isolated from the gastrocnemius and soleus muscles of previously transplanted *mdx* mice show donor-derived GFP$^+$ Pax7$^+$ satellite cells associated with GFP$^+$ myofibers. GFP is shown in green, Pax7 in red, and DAPI-stained nuclei in blue. Two representative image series are shown. (**B**) Quantitative analysis of the frequency of GFP$^+$ and GFPPax7$^+$ cells detected on single GFP$^+$ myofibers isolated from previously transplanted *mdx* muscles (gastrocnemius and soleus, n=41 individual myofibers). The majority of Pax7$^+$ cells on GFP$^+$ myofibers are GFP$^+$. (**C**) Re-isolation of GFP$^+$ SMPs from the myofiber-associated cell compartment of *mdx* mice transplanted 4 wks. previously with GFP$^+$ SMPs. The top contour plots depict events already gated for forward and side-scatter, live (calcein$^+$ propidium iodide$^-$), Sca-1$^-$CD45$^-$Mac-1$^-$ cells, and indicates the CXCR4$^+$β1-integrin$^+$ SMP population, which is further analyzed for GFP expression in the lower plot. <1% of re-isolated SMPs were GFP$^+$, in part due to low total numbers of GFP$^+$ myofibers in this particular cohort of mice (data not shown, n=4). GFP$^+$ SMPs were not detected in untransplanted control muscles (right panels). (**D**) TA muscles from *mdx* mice previously transplanted with GFP$^+$ SMPs were injured by cardiotoxin injection 4 weeks after transplantation. Analysis of donor-derived myofibers was performed 1 week after injury by direct epifluorescence microscopy. Data are presented as the mean (± SD) number of GFP$^+$ myofibers detected in the section of each engrafted muscle that contained the most GFP$^+$ myofibers (as in Figure 4). Re-injured muscles showed a significantly greater number of donor-derived myofibers (n=3), as compared to uninjured control muscles that were not re-injured (n=3). *$P < 0.05$.